SPECIAL TOPIC — International Conference on Nanoscience & Technology, China 2013

Electromagnetic wave absorbing properties and hyperfine interactions of Fe–Cu–Nb–Si–B nanocomposites*

Han Man-Gui(韩满贵)[a)†], Guo Wei(郭 韦)[a)], Wu Yan-Hui(吴燕辉)[a)], Liu Min(刘 明)[b)], and Magundappa L. Hadimani[c)]

[a)] State Key Laboratory of Electronic Thin Films and Integrated Devices, University of Electronic Science and Technology of China, Chengdu 610054, China
[b)] Analytical and Testing Center, Sichuan University, Chengdu 610064, China
[c)] Department of Electrical and Computer Engineering, Iowa State University, Ames, IA 50011, USA

(Received 4 September 2013; revised manuscript received 15 December 2013; published online 10 June 2014)

The Fe–Cu–Nb–Si–B alloy nanocomposite containing two ferromagnetic phases (amorphous phase and nanophase phase) is obtained by properly annealing the as-prepared alloys. High resolution transmission electron microscopy (HR-TEM) images show the coexistence of these two phases. It is found that Fe–Si nanograins are surrounded by the retained amorphous ferromagnetic phase. Mössbauer spectroscopy measurements show that the nanophase is the $D0_3$-type Fe–Si phase, which is employed to find the atomic fractions of resonant ^{57}Fe atoms in these two phases. The microwave permittivity and permeability spectra of Fe–Cu–Nb–Si–B nanocomposite are measured in the frequency range of 0.5 GHz–10 GHz. Large relative microwave permeability values are obtained. The results show that the absorber containing the nanocomposite flakes with a volume fraction of 28.59% exhibits good microwave absorption properties. The reflection loss of the absorber is less than −10 dB in a frequency band of 1.93 GHz–3.20 GHz.

Keywords: Mössbauer spectroscopy, magnetic permeability, nanocrystalline alloys

PACS: 33.45.+x, 75.50.Bb, 75.50.Tt. **DOI:** 10.1088/1674-1056/23/8/083301

1. Introduction

Electromagnetic properties (permittivity and permeability) of magnetic materials are important for the performances of many electronic devices operating at high frequency.[1,2] For example, the electromagnetic noise suppression in the field of electromagnetic compatibility (EMC) requires the materials having large magnetic losses or dielectric losses.[3,4] With increasing the operation frequencies of electronic devices upward to gigahertz (GHz), for instance, wireless local area network system (2.4 GHz) and active radio frequency identification label (2.45 GHz), it is imperative to develop materials which have good electromagnetic properties. As is well known, the spinel ferrites (Mn–Zn, Ni–Zn ferrites) or the hexagonal ferrites (Z-type or W-type) are the common magnetic oxides for the electromagnetic wave attenuation applications because of their high resistance and large magnetic losses arising from the natural resonance at radio frequencies (e.g. 1 MHz–300 MHz) or microwave frequencies (e.g. 500 MHz–3 GHz),[5–7] respectively. However, in comparison with ferromagnetic alloys, these ferrites have some severe shortcomings, such as a worse temperature stability, lower Curie temperature, and smaller saturation magnetization (M_s) value.[8] These shortcomings hinder their applications at high frequency or in some harsh environments. The metallic ferromagnetic alloys do not have these shortcomings; however, they suffer the large eddy current effect at high frequency, especially in the microwave frequency band. Some researchers have tried to coat the ferromagnetic particles with non-magnetic layers.[9,10] Although the non-magnetic layer can reduce the eddy current effect, the outer coating is non-ferromagnetic, which will not be helpful for attenuating the incoming EM wave via the mechanism of magnetic losses. Therefore, here we aim to develop a core–shell nanocomposite consisting of both ferromagnetic phases. As is well known, the amorphous ferromagnetic alloys have larger resistivity values than crystallized alloys.[11] If the amorphous phase forms a core shell on a nanocrystalline grain, the eddy current effect should be greatly alleviated for this nanocomposite. Fe-based nanocrystalline magnetic alloy is one of the soft ferromagnetic materials with excellent properties, which is usually used as the magnetic core material with low magnetic loss in a frequency range of around 1 kHz–1 MHz.[12–14] In this paper, we aim to develop a nanocomposite which has an amorphous phase and a nanocrystalline phase, and investigate its electromagnetic wave attenuation properties in the frequency range of 0.5 GHz–10 GHz.

2. Experimental details

$Fe_{77.8}Cu_{2.39}Nb_{3.33}Si_{16.28}B_{0.62}$ ribbons were fabricated with iron, copper, Fe–Nb alloy, and Fe–B alloy as the start-

*Project supported by the Research Fund for International Young Scientists of the National Natural Science Foundation of China (Grant No. 61250110544), the National Natural Science Foundation of China (Grant No. 61271039), the Scientific Foundation of Young Scientists in Sichuan Province, China (Grant No. 2012JQ0053), and the Program for New Century Excellent Talents in Universities, China (Grant No. NCET-11-0060).

†Corresponding author. E-mail: mangui@gmail.com

© 2014 Chinese Physical Society and IOP Publishing Ltd

ing materials. These starting materials were melted in an induction furnace. The as-prepared ribbons were prepared by a rapid quench procedure called the melt-spinning technique. The differential scanning calorimeter (DSC) measurements were carried out to find the phase transition temperatures (T_1 and T_2) with a heating rate of 5 °C/min. The as-prepared ribbons were then annealed in an argon atmosphere to obtain the nanostructured phase. X-ray diffraction (XRD) measurements (Cu K_α radiation) were conducted to examine the phases of ribbons. High resolution-transmission electron microscopy (HR-TEM, Model: TECNAI-G^2 F20) was used to investigate the nanostructures of the annealed samples. HR-TEM images and selected area electron diffraction (SAED) were taken to study the sizes of nanograins and the formation of nanophases. Mössbauer spectroscopy experiments with the transmission geometry were conducted for the annealed ribbons. The radiation source was a ^{57}Co radiation source in the rhodium (Rh) matrix. The rate of the radiation source is calibrated with a standard α-Fe foil. The Mössbauer spectra were fitted using the software called WinNormos-for-Igors®. The annealed ribbons were milled for 10 h by a planetary milling machine with ethanol as the milling dispersant, and finally they were milled into flakes. To measure the electromagnetic parameters (μ_r and ε_r), the flakes were mixed with the dispersant (paraffin) with a volume fraction of 28.59% flakes and they were made into a toroidal-shape measurement sample. The high frequency properties were measured on a vector network analyzer (Agilent 8720 ET) in the frequency range of 0.5 GHz–10 GHz based on the transmission/reflection approach by inserting the sample into a coaxial waveguide.

3. Results and discussion

In order to find the nanocrystallization temperatures for the as-prepared ribbons, DSC measurements are conducted, and the results are shown in Fig. 1(a). Two exothermal peaks can be found: one is at 530 °C (called T_{x1}) and the other is at 672 °C (called T_{x2}). T_{x1} is called the primary crystallization temperature, and T_{x2} is the secondary crystallization temperature. In order to form nanoscale grains, the as-prepared ribbons are annealed at 540 °C, which is between T_{x1} and T_{x2}. It was reported that nanoscale Fe(Si) grains can be formed.[15] The XRD patterns shown in Fig. 1(b) indicate that the as-prepared ribbons are in the amorphous state. The ribbons after the heat treatment are found to be partially nanocrystallized. XRD patterns of heat treated ribbons show that the nanocrystalline phase is α-Fe(Si). The HR-TEM images of annealed samples are shown in Fig. 2. The dark field image of TEM shows that the average grain size is about 14.38 nm (see Fig. 3(a)). Figure 2(b) shows the SAED pattern of the same sample, which manifests the coexistence of the amorphous phase and the nanophase. Multi diffraction rings are observed, which indicate the formation of crystalline grains. The halo in the SAED pattern indicates the existence of the amorphous phase. HR-TEM images of these two phases are shown in Figs. 2(c) and 2(d). The spacing of the (220) plane of Fe–Si nanograins is found to be about 2.0 Å (see Fig. 2(c)). Crystal defects are also found as marked in the zones by "A" and "B" in Fig. 2(c). More importantly, it is evidenced in Fig. 2(d) that the nano grains are surrounded by the amorphous phase; such a core–shell nanostructure is what we intend to obtain and is believed to be helpful to alleviate the eddy current effect at GHz frequency. For the Fe(Si) alloy, the occupancy of Fe and Si atoms in the crystal lattice can be random or ordered.[16] For an ordered Fe–Si alloy, the occupancy possibilities of the Fe atom vary with the content of Si atoms. The Mössbauer spectroscopy technique is a powerful tool for studying such atomic occupancy differences. For instance, Fe atoms exist in both phases in the nanocomposite under study, it is easy and reliable to find the atomic fraction of Fe atoms in the respective phase.

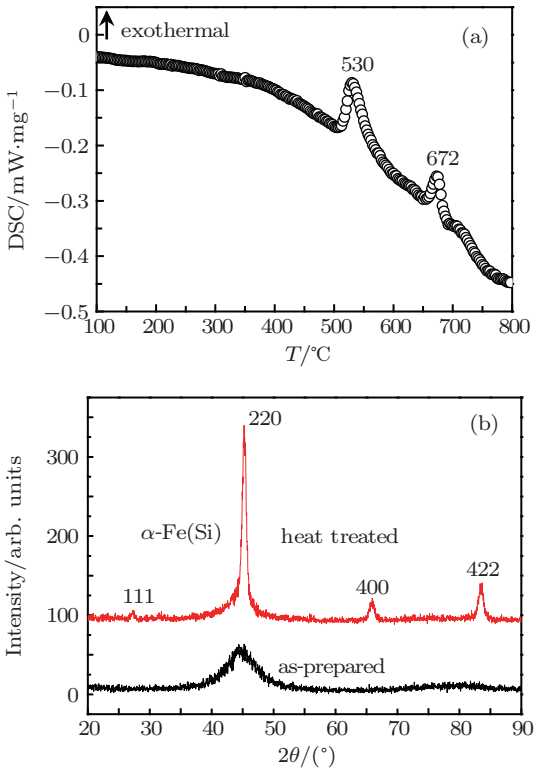


Fig. 1. (color online) (a) DSC–T curve and (b) XRD patterns.

As is well known, there are two ferromagnetic phases inside the alloy: one is the amorphous ferromagnetic phase, in which Fe atoms are distributed randomly, and the other phase is D0$_3$-type Fe (Si) nanograin. The Mössbauer spectrum is fitted by a combination of the component related to the distribution of hyperfine fields and discrete spectral components with narrow lines originating from various Fe positions in the D0$_3$-type Fe–Si lattice. For our nanocomposite, four kinds of Fe

atom environments can be classified according to Fig. 2(d) and the schematic presentation shown in Fig. 3(a). The first case (I) is that Fe atoms are located in Fe–Si nano grains, which can be represented by several discrete sextets. The second case (II) is that Fe atoms constitute the outer surface of a nanograin. The third case (III) is that Fe atoms are situated in the interface between two nanograins or between the nanograin and the amorphous phase. The fourth case (IV) is that Fe atoms are located in the amorphous matrix with a disordered atomic arrangement, which do not directly contact the nano grains. The second case (II) and the third case (III) are usually classified as the interface zone.[17] Fe atoms in this zone have randomly disordered neighboring atoms. Therefore, a distribution hyperfine interaction model should be used to fit the scenario for Fe atoms located in the regions of II, III, and IV.

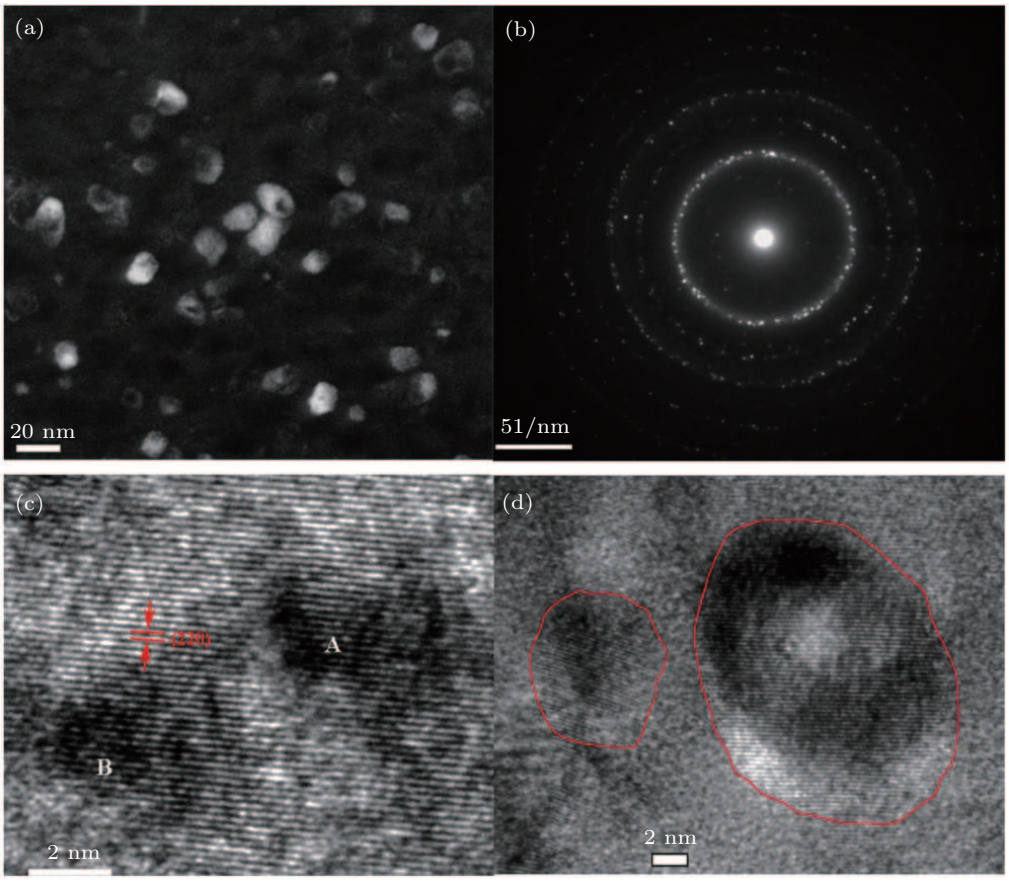


Fig. 2. (color online) TEM images: (a) dark field image; (b) SAED pattern; (c) and (d) high resolution images.

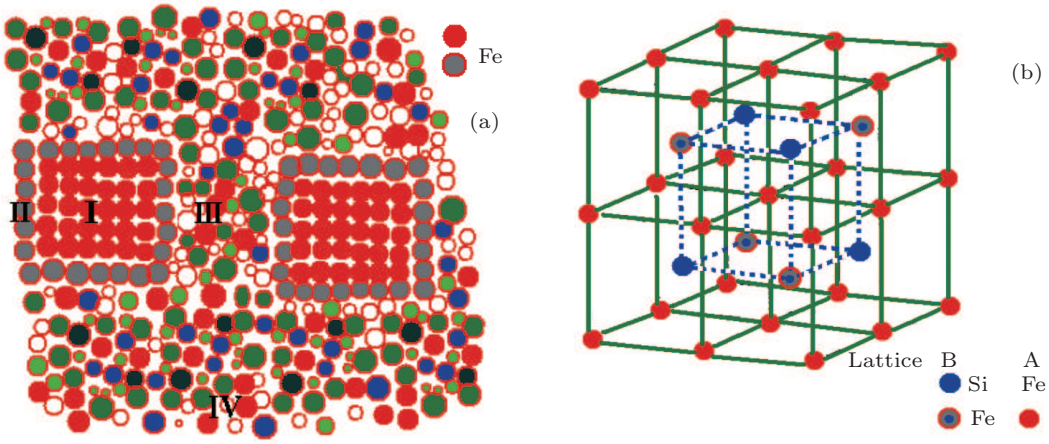


Fig. 3. (color online) Schematic representations of (a) Fe environments in the nanocomposite and (b) the D03-type Fe–Si superlattice.

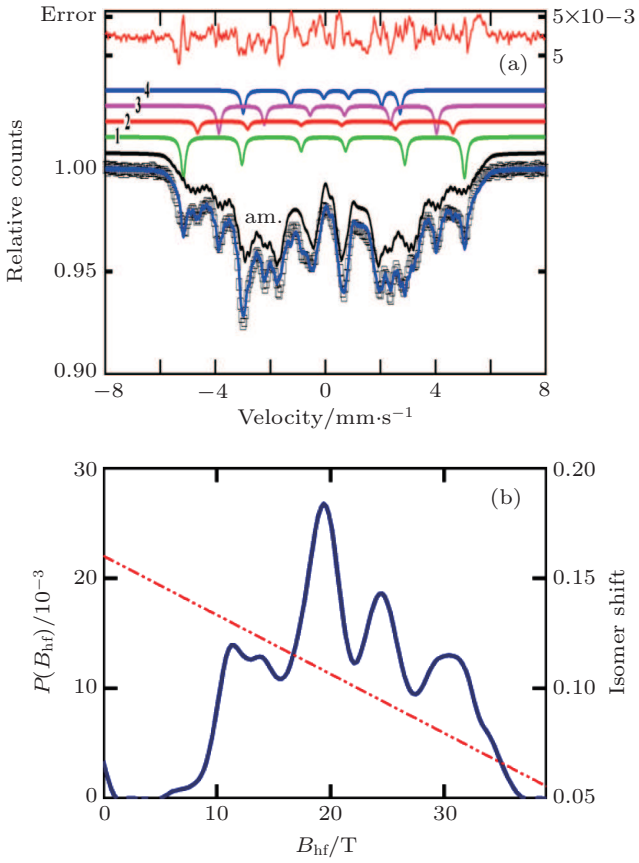


Fig. 4. (color online) Mössbauer spectra of Fe–Cu–Nb–Si–B nanocomposites.

The superlattice of Fe–Si is shown in Fig. 3(b), which consists of an "A" lattice with sites occupied by Fe atoms, and a "B" lattice with sites occupied by Fe and Si atoms. For each atom in the "B" lattice, it has eight Fe atoms as its nearest neighbors. For each Fe atom in the "A" lattice, it has a varying number of nearest-neighbor Fe or Si atoms depending on the Si concentration. The Mössbauer spectra of the Fe-based nanocrystalline alloy are shown in Fig. 4. Clearly, the fittings and the experimental data of the Mössbauer spectrum agree very well (see Fig. 4(a)). The fitting results show that the Mössbauer spectrum can be resolved into four discrete sextets and one broad subspectrum labelled as "am". The four resolved discrete sextets (labelled as 1–4 respectively) represent the four possibilities of the nearest neighboring for ^{57}Fe atoms in the D03-type Fe–Si superlattice. The fitting results are shown in Table 1. The hyperfine magnetic fields ($B_{\rm hf}$) we have obtained for these four discrete sextets are very close to those reported by others.[16,18] "1" denotes the case of eight Fe atoms as the nearest neighbors of a resonant ^{57}Fe atom, which can be simply marked as "8Fe0Si". In the same way, "2" denotes the case of "6Fe2Si", "3" denotes the case of "5Fe3Si", and "4" denotes the case of "4Fe4Si". For each kind of neighboring occasion, the hyperfine magnetic field acting on the resonant ^{57}Fe atoms is given in Table 1. As for the ^{57}Fe atoms in the zone having random neighboring atoms (Fe, Cu, Nb, Si, and B), the distribution of hyperfine interaction parameters ($B_{\rm hf}$ and isomer shift) is shown in Fig. 4(b). Clearly, the value of the hyperfine magnetic field mainly falls within the range of 10 T–40 T. The distribution of hyperfine interactions originates from two regions, i.e. regions II and III shown in Fig. 3(a). The relative areas for each sextet reveal the possibilities of each surrounding, which are also given in Table 1. The relative atomic fractions of Fe atoms in the amorphous phase and nanophase are 42.635% and 57.365% respectively, as indicated in Table 1.

Table 1. Fitting results of Mössbauer spectrum.

	Amorphous	S1	S2	S3	S4
$B_{\rm hf}$/T	21.149	31.684	28.776	24.525	17.677
Percentage/%	42.635	18.511	9.771	15.207	13.877

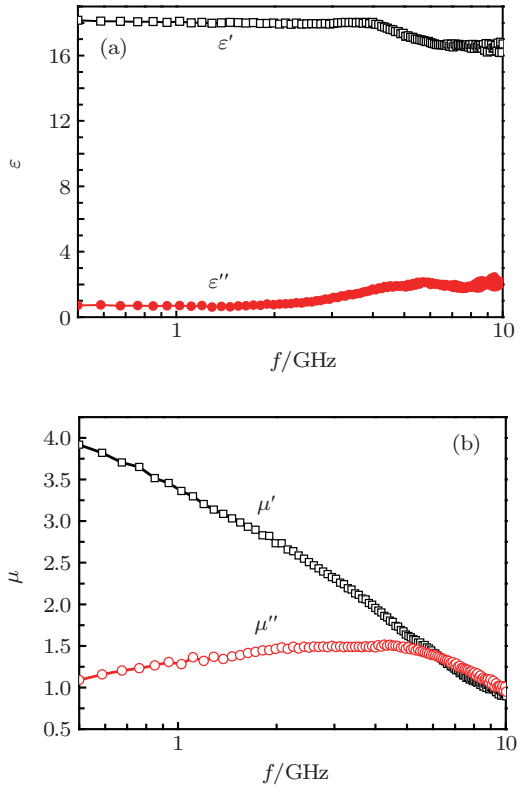


Fig. 5. (color online) Microwave permittivity (a) and permeability (b) spectra of Fe-based nanocomposites.

The electromagnetic properties of Fe–Cu–Nb–Si–B nanocomposites are shown in Fig. 5. The dependences of relative complex permittivity on frequency is shown in Fig. 5(a). It is found that the variation of permittivity is not obvious in the frequency range of 0.5 GHz–4 GHz. Besides, the high frequency dielectric loss is insignificant in this frequency range. However, it is observed that the complex permeability significantly varies with frequency. A wide magnetic loss peak (i.e. $\mu'' \sim f$) is obviously seen in Fig. 5(b). Once the dependences of permittivity and permeability on frequency have been measured, the electromagnetic wave (EM) absorption of an absorber containing these ferromagnetic flakes with the reported nanocomposite features can be evaluated by the follow-

ing equations, and the properties of EM absorption are characterized by the reflection loss (RL):[19–21]

$$Z_{\text{in}} = Z_0\sqrt{\mu_{\text{r}}/\varepsilon_{\text{r}}}\tanh\left\{\text{j}\left(\frac{2\pi ft}{c}\right)\sqrt{\mu_{\text{r}}\varepsilon_{\text{r}}}\right\}, \quad (1)$$

$$RL = 20\log|(Z_{\text{in}} - Z_0)/(Z_{\text{in}} + Z_0)|, \quad (2)$$

where "Z_{in}" is the input impedance of the absorber, "Z_0" is the impedance of the free space, "t" is the thickness of an absorber, and "c" is the speed of light. Figure 6 shows that when the thickness of the absorber is 4 mm, good electromagnetic wave attenuation can be achieved. In the frequency range of 1.93 GHz–3.20 GHz, the value of RL is less than −10 dB.

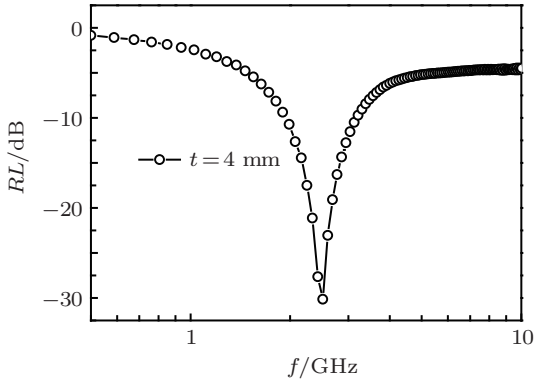


Fig. 6. Microwave absorption property of the Fe-based nanocomposite.

4. Conclusions

The as-prepared Fe–Cu–Nb–Si–B alloys are found to be amorphous. A nanocomposite containing core–shell nanostructures is obtained by heat treatments. The core is composed of Fe–Si nanograins. The shell is the amorphous phase. Both the core and shell are ferromagnetic, which is verified by Mössbauer measurements. HR-TEM results show that the average grain size of the nanophase is about 14.38 nm. Mössbauer spectrum results show that the nanograins are of Fe–Si alloy with the $D0_3$-type superlattice structure and an atomic fraction of 57.365% for Fe atoms. Large microwave permeability values are found in the nanocomposites. In the frequency range of 1.93 GHz–3.20 GHz, the absorber containing the flakes with the nanostructures shows a good electromagnetic wave attenuation property when the absorber has a thickness of 4 mm.

References

[1] Kazimierczuk M K 2009 *High Frequency Magnetic Components* (John Wiley & Sons, Ltd)
[2] Li S, Liu M, Lou J, Xing X, Wu J, Hu Y, Cai X, Xu F, Sun N X and Duh J G 2013 *J. Nanosci. Nanotech.* **13** 1091
[3] Han Y, Cheung G, Li A, Sullivan C R and David J P 2012 *IEEE Trans. Power Electr.* **27** 425
[4] Abbas S M, Chandra M, Verma A, Chatterjee R and Goel T C 2006 *Composites Part A* **37** 2148
[5] Nakamura T 2000 *J. Appl. Phys.* **88** 348
[6] Korolev K A, McCloy J S and Afsar M N 2012 *J. Appl. Phys.* **111** 07E113
[7] Nakamura T and Hankui E 2003 *J. Magn. Magn. Mater.* **257** 158
[8] Goldman Alex 2006 *Modern Ferrites Technology*, 2nd edn. (Springer)
[9] Yan L G, Wang J B, Han X H, Ren Y, Liu Q F and Li F S 2010 *Nanotechnology* **21** 095708
[10] Yang X C, Liu R J, Shen X Q, Song F Z, Jing M X and Meng X F 2013 *Chin. Phys. B* **22** 058101
[11] Chiriac H and Ovari T 1996 *Prog. Mater. Sci.* **40** 333
[12] Varga L K and Kovacs G 2012 *IEEE Trans. Magn.* **48** 1360
[13] Kuzmann E, Stichleutner S, Sapi A, Klencsar Z, Oshtrakh M I, Semionkin V A, Kubuki S, Homonnay Z and Varga L K 2013 *Hyperfine Interact.* **219** 63
[14] Füzerová J, Füzer J, Kollár P, Bureš R and Fáberová M 2013 *J. Magn. Magn. Mater.* **345** 77
[15] McHenry M E, Willard M A and Laughlin D E 1999 *Prog. Mater. Sci.* **44** 291
[16] Stearns M B 1963 *Phys. Rev.* **129** 1136
[17] Miglierini M and Greneche J M 1997 *J. Phys.: Condens. Matter* **9** 2303
[18] Kopcewicz M 2005 *Handbook of Advanced Magnetic Material*, Vol. II (Beijing: Tsinghua University Press)
[19] Naito Y and Suetake K 1971 *IEEE Trans. Microwave Theory Technol.* **19** 65
[20] Han M, Liang D and Deng L 2011 *Appl. Phys. Lett.* **99** 082503
[21] Lu H P, Han M G, Cai L and Deng L J 2011 *Chin. Phys. B* **20** 060701